

Above-threshold ionization of xenon atoms in a bichromatic phase-controlled laser field of linear and circular polarizations

Jingtao Zhang,¹ Shaohui Li,^{1,2} and Zhizhan Xu¹

¹Laboratory for High Intensity Optics, Shanghai Institute of Optics and Fine Mechanics, Chinese Academy of Sciences, P.O. Box 800-211, Shanghai 201800, People's Republic of China

²Department of Physics, Shantou University, Shantou 515063, People's Republic of China

(Received 19 November 2003; revised manuscript received 15 December 2003; published 17 May 2004)

Using a nonperturbative scattering theory, we study the photoionization of xenon atoms irradiated by a bichromatic laser field of linear and circular polarizations. The bichromatic laser field is modulated in such a way that it comprises an infinite sequence of identical, one-cycle laser pulses. The photoelectron angular distribution (PAD) in such a field is inversion asymmetric and depends on the phase difference between laser modes, the laser polarization and intensity, and the kinetic energy of photoelectrons. By investigating the broadening effect in the PADs of lower-order peaks, we show that one can perform an effective control on the motion of electrons of high kinetic energy.

DOI: 10.1103/PhysRevA.69.053410

PACS number(s): 32.80.Rm, 42.50.Hz, 42.50.Vk, 42.50.Ct

I. INTRODUCTION

Photoionization of atoms is one of the most attractive topics in intense-field studies. Photoionization of atoms in intense field is characterized by above-threshold ionization (ATI), which means an atom absorbing more photons than are necessary for its ionization. This phenomenon was first observed in 1979 [1], and in the following two decades, many notable progress has been achieved both in experimental measurements and in theoretical descriptions [2–7].

Photoelectron angular distributions (PADs) are an important tool both in experimental researches and in the comparison of experimental observations with theoretical studies. It is found that the PADs in monochromatic laser field are azimuthal isotropic for circular polarization and are fourfold symmetric for linear polarization [4], and the PADs in bichromatic laser field have quite different features from those in monochromatic laser field and are very sensitive to the phase difference among modes [8–13].

On the other hand, recent developments in laser technology have made it possible to produce high intensity laser pulses of few optical cycles [14]. In such laser pulses, the initial phase of the carrier wave with respect to the pulse envelope (the so-called carrier-envelope phase, CE phase) plays an important role [6,7,15,16]. A few-cycle laser pulse consists of many frequency components, thus can be treated as a multimode laser field [17].

In this paper, we study the photoionization of xenon atoms in a bichromatic laser field. The two modes of the laser field are consisted of a fundamental frequency ω and its second harmonic, and they are of the same propagation direction and polarization. Different from the related theoretical study on two-color ATI [8,9], the electric strength of the fundamental mode is twice that of the harmonic mode. In such a modulation manner, the synthesized electric field behaves as an infinite sequence of identical, one-cycle laser pulses, which can be shown as follows:

$$\begin{aligned} \mathbf{E}(t) &= \mathbf{E}_0[2 \sin(\omega t - \phi) - \sin(2\omega t - 2\phi)]/4 \\ &= \mathbf{E}_0 \sin^2(\omega t/2 - \phi) \sin(\omega t - \phi), \end{aligned}$$

where \mathbf{E}_0 is the peak value of the synthesized electric field and ϕ is the phase difference between modes. After a time displacement $t \rightarrow t + 2\phi/\omega$ and introducing $T = 2\pi/\omega$, the electric field can be rewritten as

$$\mathbf{E}(t) = \mathbf{E}_0 \sin^2(\pi t/T) \sin(\omega t + \phi). \quad (1)$$

In such a field, the first term can be regarded as the envelope of an infinite sequence of one-cycle pulses, while the second term acts as the carrier wave (see Fig. 1). Thus, the synthesized field corresponds to an infinite sequence of one-cycle pulses, each of which shares a common phase ϕ . Throughout this paper, we term the peak intensity of the synthesized

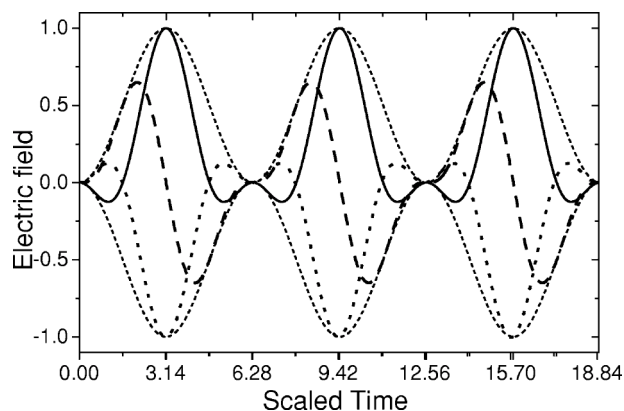


FIG. 1. Time variation of the electric field as a function of time for several CE phases: $\phi = -0.5\pi$ (solid line), 0 (dashed line), and 0.5π (dotted line), respectively; short dashed lines show the envelope of the pulses. The scaled time denotes ωt .

one-cycle pulses as the laser intensity and the phase difference ϕ as the CE phase.

This study is based on a nonperturbative scattering theory of ATI developed by Guo, Aberg, and Crasemann [18], which treats the Volkov states as intermediate states while the final state of ATI is an electron-photon plane wave. The PADs and the photoelectron spectra in the bichromatic field are obtained for different polarizations. We will show the variation of PADs with the CE phase, the polarization, and the kinetic energy of photoelectron.

This paper is organized as follows: the wave function of the photoelectron moving in the bichromatic field and the ionization-rate formula are given in Sec. II; the numerical results of various laser intensities and CE phases are presented in Sec. III; and IV is for conclusions and discussions.

II. IONIZATION-RATE FORMULA

The state of an electron moving in a bichromatic laser field is described by a two-mode Volkov state as follows ($\hbar=1, c=1$):

$$|\Psi_\mu\rangle = V_e^{-1/2} \sum_{j_1 j_2} \exp\{i[\mathbf{P} + (u_{p1} - j_1)\mathbf{k}_1 + (u_{p2} - j_2)\mathbf{k}_2] \cdot \mathbf{r}\} \\ \times \mathcal{X}_{j_1 j_2}(z) |n_1 + j_1, n_2 + j_2\rangle, \quad (2)$$

where V_e denotes the electron normalization volume, \mathbf{P} is the electron's momentum in the Volkov state, and $\mathbf{k}_1, \mathbf{k}_2$ are the wave vectors of two laser modes, respectively; n_i is the background photon numbers in the i th mode, and j_i denotes the number of transferred photons. In Eq. (2), the ponderomotive parameters are defined as

$$u_{p1} = \frac{e^2 \Lambda_1^2}{m_e \omega_1}, \quad u_{p2} = \frac{e^2 \Lambda_2^2}{m_e \omega_2},$$

where $2\Lambda_i$ is classical amplitude of the i th mode, and $\Lambda_1 = 4\Lambda_2$, $\omega_1 = \omega$, $\omega_2 = 2\omega$, thus $u_{p2} = u_{p1}/32$. The two-mode generalized phased Bessel (GPB) function $\mathcal{X}_{j_1 j_2}(z)$ is defined as [9]

$$\mathcal{X}_{j_1 j_2}(z) = \sum_{q_1 \dots q_4} X_{-j_1 + 2q_1 + q_3 + q_4}(\zeta_1) X_{-j_2 + 2q_2 + q_3 - q_4}(\zeta_2) X_{-q_1}(z_1) \\ \times X_{-q_2}(z_2) X_{-q_3}(z_3) X_{-q_4}(z_4),$$

where the sum is performed over $-\infty < q_i (i=1, \dots, 4) < \infty$, and $X_n(z)$ is the phased Bessel function related to the ordinary Bessel function as

$$X_n(z) = J_n(|z|) e^{in \arg(z)}.$$

The arguments of the GPB function are defined as

$$\zeta_1 = \frac{2|e|\Lambda_1}{m_e \omega_1} \mathbf{P} \cdot \boldsymbol{\epsilon}_1, \quad \zeta_2 = \frac{2|e|\Lambda_2}{m_e \omega_2} \mathbf{P} \cdot \boldsymbol{\epsilon}_2, \\ z_1 = \frac{1}{2} u_{p1} \boldsymbol{\epsilon}_1 \cdot \boldsymbol{\epsilon}_1, \quad z_2 = \frac{1}{2} u_{p2} \boldsymbol{\epsilon}_2 \cdot \boldsymbol{\epsilon}_2, \quad (3) \\ z_3 = \frac{2e^2 \Lambda_1 \Lambda_2 \boldsymbol{\epsilon}_1 \cdot \boldsymbol{\epsilon}_2}{(\omega_1 + \omega_2) m_e}, \quad z_4 = \frac{2e^2 \Lambda_1 \Lambda_2 \boldsymbol{\epsilon}_1 \cdot \boldsymbol{\epsilon}_2^*}{(\omega_1 - \omega_2) m_e},$$

where $\boldsymbol{\epsilon}_k (k=1, 2)$ is the polarization vector of the k th mode defined as

$$\boldsymbol{\epsilon}_k = [\boldsymbol{\epsilon}_x \cos(\xi/2) + i \boldsymbol{\epsilon}_y \sin(\xi/2)] e^{i\phi_k}, \\ \boldsymbol{\epsilon}_k^* = [\boldsymbol{\epsilon}_x \cos(\xi/2) - i \boldsymbol{\epsilon}_y \sin(\xi/2)] e^{-i\phi_k}, \quad (4)$$

and ξ monitors the polarization degree such that $\xi=0$ denotes linear polarization and $\xi=\pi/2$ circular polarization; ϕ_k is the phase angle of the k th mode,

$$\phi_1 = \pi, \quad \phi_2 = -\phi.$$

The polarization vectors satisfy the following relations:

$$\boldsymbol{\epsilon}_j \cdot \boldsymbol{\epsilon}_k = \cos(\xi) e^{i(\phi_j + \phi_k)}, \quad \boldsymbol{\epsilon}_j \cdot \boldsymbol{\epsilon}_k^* = e^{i(\phi_j - \phi_k)}. \quad (5)$$

The transition matrix element is given by [18]

$$T_{fi} = \sum_{\epsilon_\mu = \epsilon_i} \langle \phi_f(\mathbf{r}); m_1, m_2 | \Psi_\mu \rangle \langle \Psi_\mu | V(\mathbf{r}) | \Phi_i(\mathbf{r}); l_1, l_2 \rangle, \quad (6)$$

where $\phi_f(\mathbf{r})$ is the final plane wave for a free electron, $\Phi_i(\mathbf{r})$ is the state of an initial bound electron with binding energy E_b ; l_i and $m_i (i=1, 2)$ are, respectively, the initial and final numbers of photons in the i th mode; and $V(\mathbf{r})$ is the interaction Hamiltonian:

$$V(\mathbf{r}) = \frac{-e}{2m_e} [(-i\nabla) \cdot \mathbf{A} + \mathbf{A} \cdot (-i\nabla)] + \frac{e^2 \mathbf{A}^2}{2m_e}, \quad (7)$$

where \mathbf{A} is the quantized vector potential of the bichromatic field:

$$\mathbf{A}(-\mathbf{k} \cdot \mathbf{r}) = \sum_{j=1}^2 g_j (\boldsymbol{\epsilon}_j e^{i\mathbf{k}_j \cdot \mathbf{r}} a_j + \boldsymbol{\epsilon}_j^* e^{-i\mathbf{k}_j \cdot \mathbf{r}} a_j^\dagger), \quad (8)$$

where $g_j = (2V_j \omega_j)^{-1/2}$, V_j is the normalization volume of the j th photon mode. By means of the Volkov state given in Eq. (2), the transition matrix element is worked out to be

$$T_{fi} = V_e^{-1/2} \sum_{j_1 j_2} [(u_{p1} - j_1) \omega_1 + (u_{p2} - j_2) \omega_2] \\ \times \mathcal{X}'_{j_1 j_2}(z_f) \mathcal{X}_{j_1 j_2}(z_f)^* \Phi_i(\mathbf{P}_f), \quad (9)$$

where $j_i = l_i - n_i$, $j'_i = m_i - n_i (i=1, 2)$, and $\Phi_i(\mathbf{P}_f)$ is Fourier transformation of the initial wave function $\Phi_i(\mathbf{r})$, and \mathbf{P}_f is the final momentum of photoelectron. In Eq. (9), the ζ_i variables of the GPB function are reduced to

$$\zeta_{1f} = \frac{2|e|\Lambda_1}{m_e \omega_1} \mathbf{P}_f \cdot \boldsymbol{\epsilon}_1, \quad \zeta_{2f} = \frac{2|e|\Lambda_2}{m_e \omega_2} \mathbf{P}_f \cdot \boldsymbol{\epsilon}_2, \quad (10)$$

while the z_i variables are kept unchanged.

The total transition rate is given by

$$W = \frac{V_e}{(2\pi)^3} \int d\mathbf{P}_f 2\pi \delta(\mathcal{E}_i - \mathcal{E}_f) |T_{fi}|^2. \quad (11)$$

Expanding the overall energy conservation relation as

$$\begin{aligned} \delta(\mathcal{E}_i - \mathcal{E}_f) &= (m_e/2\omega)^{1/2} (q - \epsilon_b)^{-1/2} \delta(P_f - (2m_e\omega)^{1/2} \\ &\quad \times (q - \epsilon_b)^{1/2}), \end{aligned} \quad (12)$$

where $\epsilon_b = E_b/\omega$ and $q = q_1 + 2q_2$ with $q_i = l_i - m_i$ ($i = 1, 2$), we express the photoelectron rate in the bichromatic laser field as

$$\begin{aligned} \frac{d^2W}{d\Omega_{P_f}} &= \frac{(2m_e^3\omega^5)^{1/2}}{(2\pi)^2} (q - \epsilon_b)^{1/2} |\Phi_i(\mathbf{P}_f)|^2 \left| \sum_{q_1, q_2} [(u_{p1} - q_1) \right. \\ &\quad \left. + 2(u_{p2} - q_2)] \sum_{j_1, j_2} \mathcal{X}_{j_1 - q_1, j_2 - q_2}(z_f) \mathcal{X}_{j_1, j_2}(z_f)^* \right|^2, \end{aligned} \quad (13)$$

where $d\Omega_{P_f} = \sin\theta_f d\theta_f d\phi_f$ is the differential solid angle of the final photoelectron, here θ_f and ϕ_f are the scattering angle and the azimuthal angle, respectively; q is related to the final kinetic energy of photoelectron, thus can be used to denote the order of an ATI peak. The emission rate of a given ATI peak is got by integrating over the solid angle, and the PAD denotes the emission rate at different azimuthal angles in polarization plane defined by $\theta_f = 0.5\pi$.

For a monochromatic field, the photoelectron rates in a pair of two opposite directions always equal to each other, which is termed as inversion symmetry in PADs. In bichromatic laser fields, the PADs are not always inversion symmetric yet. Notice that most experimental observations are performed in the polarization plane, the space reflection means ϕ_f being replaced by $\phi_f + \pi$, which results in a phase change in the GPB function as follows:

$$\mathcal{X}_{j_1, j_2}(z_f | \phi_f + \pi) = (-1)^{j_1 + j_2} \mathcal{X}_{j_1, j_2}(z_f | \phi_f). \quad (14)$$

Thus the transition rate subjected to the space reflection changes to

$$\begin{aligned} \frac{d^2W}{d\Omega_{P_f}} &= \frac{(2m_e^3\omega^5)^{1/2}}{(2\pi)^2} (q - \epsilon_b)^{1/2} |\Phi_i(\mathbf{P}_f)|^2 \\ &\quad \times \left| \sum_{q_1, q_2} (-1)^{q_1 + q_2} [(u_{p1} - q_1) + 2(u_{p2} - q_2)] \right. \\ &\quad \left. \times \sum_{j_1, j_2} \mathcal{X}_{j_1 - q_1, j_2 - q_2}(z_f) \mathcal{X}_{j_1, j_2}(z_f)^* \right|^2. \end{aligned} \quad (15)$$

The space reflection leads to an additional term $(-1)^{q_1 + q_2}$ in the transition rate, as compared with Eq. (13). Whether the transition rate changes or not is determined by the sum of q_i . We identify one set of q_i that satisfies $q\omega = q_1\omega_1 + q_2\omega_2$ for a fixed q as a transition channel. The phase of each channel varies with the value of q_i , thus different channels are of different phases. When several channels are involved to form an ATI peak, the interference among channels will affect the ionization rate. Then we conclude that the inversion asymmetry is resulted from the interference among transition channels.

The frequency spectrum of long pulses is highly focused on the central frequency component, thus can be treated as a monochromatic laser field, correspondingly, only one channel exists to form an ATI peak and the PADs are inversion symmetric. A short pulse has a broad frequency spectrum. An electron may absorb photons from different frequency components for its ionization, then many transition channels are involved to form an ATI peak and the PAD is not always inversion symmetric yet. The inversion asymmetry is not related to the laser polarization, but the PADs vary with the laser polarization. The inversion-asymmetric PADs show quite different characters for different polarizations.

III. NUMERICAL RESULTS

By means of the transition-rate formula in Eq. (13), we obtain the PADs and the photoelectron spectra for linear and circular polarizations. The synthesized field is of peak intensity varying from 10^{13} to 10^{14} W/cm², and of central wavelength 800 nm. In our calculations, the wave function is chosen as that of the outermost shell ($5P_{3/2}$) of xenon atom with binding energy 12.1 eV.

We first calculate the PADs in a single transition channel for circular and linear polarizations. Our calculations show that the PADs in a single channel are isotropic for circular polarization and are fourfold symmetric for linear polarization, and the PADs do not depend on the CE phase. This result confirms the earlier studies [4]. We then calculate the PADs including all the possible transition channels according to Eq. (13). Some results were shown below.

Generally, the PADs are inversion asymmetric and depend on the CE phase. The inversion-asymmetric PADs have a maximum and a minimum relating to the CE phase, which forms the foundation of CE control to the motion of photoelectrons. Although we have shown that the inversion asymmetry arises from the interference among transition channels, a more direct picture is that the inversion asymmetry reflects the asymmetric distribution of the electric field in the pulse envelope. Because the electric-field distribution varies with the laser polarization, the main features of PADs and their dependence on the CE phase are distinct for different polarizations.

A. PADs in circularly polarized fields

Figure 2 is the calculated PADs of the first three ATI peaks for several CE phases in a circularly polarized laser field of peak intensity 3×10^{13} W/cm². It is clear that the PADs are not isotropic yet, and the direction of the maximal ionization varies with the CE phase. Take the PADs of the first peak as an example, the maximal ionization appears at $\phi_f = \pi$, 0.5π , and 0 when the CE phase $\phi = 0$, 0.5π , and π , respectively. Other ATI peaks show similar distributions at the chosen intensities. Several points about the PADs should be mentioned: First, the ejected electrons take up a wide range; second, the PADs are inversion asymmetric for all the CE phases and are symmetric about an axis rotating with the CE phase; and last, the maximal ionization rate is kept constant for various CE phase, but the position of the maximum

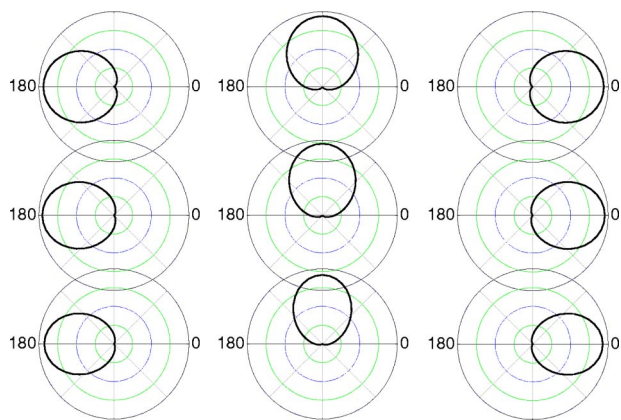


FIG. 2. The polar plots of the calculated PADs for the first (in top row), the second (in middle row), and the third (in bottom row) ATI peaks for several CE phases in a circularly polarized field. The plots in each column are of the same CE phase: $\phi=0$ for the left column, $\phi=0.5\pi$ for the middle column, and $\phi=\pi$ for the right column. The peak intensity of the synthesized field is chosen as $3 \times 10^{13} \text{ W/cm}^2$.

varies with the CE phase. This phenomenon reflects the fact that the maximal field strength of the synthesized circularly polarized pulse keeps constant, but the position of the maximal electric-field strength varies with the CE phase.

Since the photoelectron rate is related to the simultaneous electric-field strength via a highly nonlinear manner, the photoelectron rate rises quickly with the increasing laser intensity, and the PADs also vary with the intensity of electric field. In Fig. 3, we show the PADs of the first three ATI peaks in a circularly polarized field of higher intensity. Compared with the PADs at lower intensities, as shown in Fig. 2, the PADs at higher intensities are a little narrow around their symmetric axis. The difference is subtle for lower-order peaks, but is clear for higher-order peaks. This phenomenon is obvious after a comparison made on the PADs of the third peak.

B. PADs in linearly polarized fields

Now we turn to the case of linear polarization. In linearly polarized laser fields, rescattering of the ionized electron by

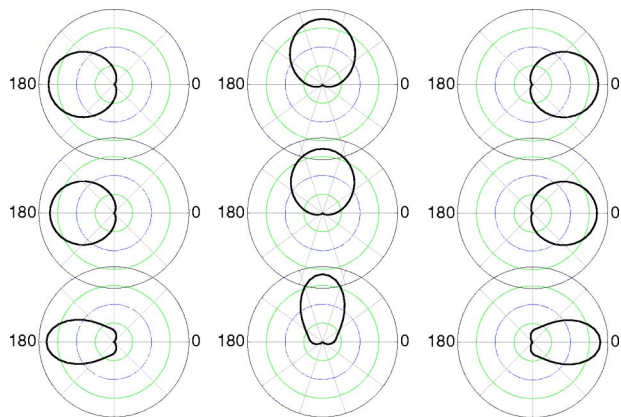


FIG. 3. The polar plots of the calculated PADs of the first three ATI peaks in a circularly polarized laser field of intensity $7 \times 10^{13} \text{ W/cm}^2$. Other conditions are the same as in Fig. 2.

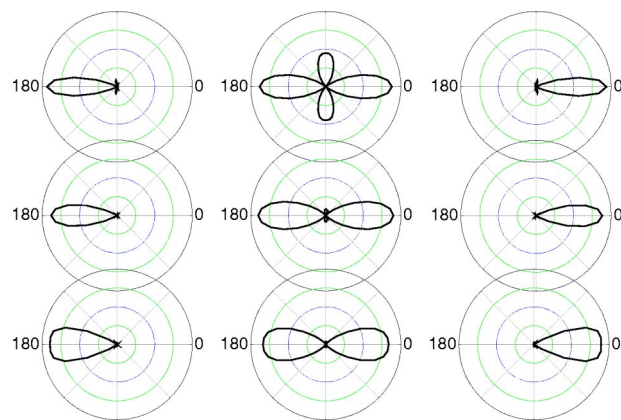


FIG. 4. The polar plots of the calculated PADs of the third (in top row), the fourth (in middle row), and the fifth (in bottom row) ATI peaks in a linearly polarized laser field. The CE phase in each column is of the same value, same as those in Fig. 2. The laser intensity is chosen as $7 \times 10^{13} \text{ W/cm}^2$. The azimuth denotes the angle between the polarization vector and detection direction.

its parent ion might be evident [8]. At the laser intensities used in this paper, the rescattering contributes mainly to the photoelectrons of high kinetic energy ($>20 \text{ eV}$) [19]. For we focus on the photoelectrons of relatively lower kinetic energy, the influence of rescattering effect is subtle. Thus, the rescattering was not specially treated in this paper.

Figure 4 shows the calculated PADs of the third, the fourth, and the fifth ATI peaks in a linearly polarized laser field at intensity $7 \times 10^{13} \text{ W/cm}^2$ for several CE phases. It is clear that all the PADs are peaked along the polarization vector and are symmetric about the polarization vector. Although the PADs are inversion asymmetric almost for all CE phases, it is found that the PADs are inversion symmetric for some special values of the CE phase, such as 0.5π shown in the middle column of Fig. 4. The symmetry in the PADs reflects the symmetry in the electric-field distributions.

Since electrons in the electric field move mainly along the polarization vector, it is expected that electrons ejected outside the laser field are mostly distributed along the polarization vector and form the main lobe of PADs. The jetlike structures sticking out the main lobes arise from the inherent property of photoionization[20]. Although the jets shrink with the increasing kinetic energy of photoelectron, detailed studies show more jets existing in high-order peaks. In the inversion asymmetric PADs, the jets become very small thus the fraction of electrons moving outside the main lobes is negligible.

Several points should be mentioned: First, the ionization rate in a linearly polarized laser field is much higher than that in a circularly polarized field of equal intensity; second, most PADs are highly peaked along the polarization vector, and the maximum rate varies with the CE phase; and last, the PADs are always symmetric about the polarization axis, and are fourfold symmetric for some special CE phases.

In order to show clearly the variation of the maximal ionization rate with CE phase in a linearly polarized field, we depict in Fig. 5 the maximal ionization rate in the two poles of the polarization vector as a function of CE phase at inten-

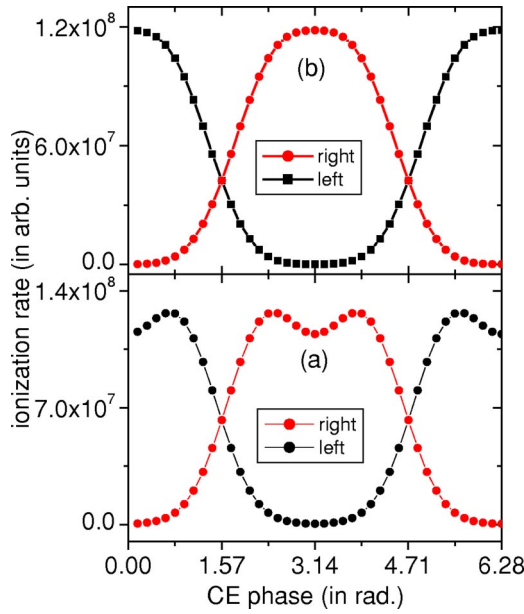


FIG. 5. Variation of the ionization rate in the two poles of the polarization vector in a linearly polarized laser field at intensity $7 \times 10^{13} \text{ W/cm}^2$ for (a) the third and (b) the fourth peak. Left means the azimuthal angle $\phi_f = \pi$ and right means $\phi_f = 0$.

sity of $7 \times 10^{13} \text{ W/cm}^2$. Noting that the maximal ionization rate for circular polarization is kept unchanged for various CE phases, the dependence of the ionization rate on the laser polarization is obvious.

C. The broadening effect in PADs

Our calculations show that the PADs for lower-order peaks are relatively broad while those of higher-order peaks are a little narrow. This tendency is more clear in linearly polarized fields, as shown in Fig. 6 for the first four ATI peaks at intensity 10^{13} W/cm^2 with $\phi = 0.5\pi$. From Fig. 6 we see that the PAD for the first peak is almost isotropic, and ratio of the maximal ionization rate to the minimal ionization

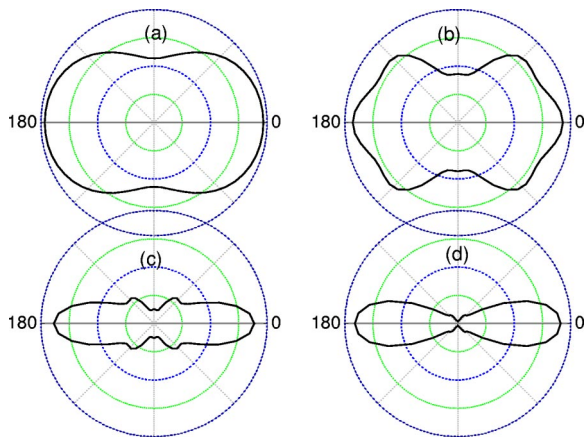


FIG. 6. The polar plots of the calculated PADs in a linearly polarized laser field at laser intensity 10^{13} W/cm^2 for (a) the first, (b) the second, (c) the third, and (d) the fourth peak. The CE phase is chosen as $\phi = 0.5\pi$.

rate is about 0.6, while that of the second peak is about 0.45, and the PADs for the third and the fourth peaks are highly peaked along the polarization vector. This means that the PADs of lower-order peaks tend to be isotropic, which we term as the broadening effect in the PADs of lower-order ATI peaks. This effect was first observed in the ATI of xenon atoms by Freeman *et al.* [21].

Our calculations confirm the broadening effect of low-order ATI peaks and show that when the laser intensity increases from 10^{13} W/cm^2 to $4 \times 10^{13} \text{ W/cm}^2$, the broadening effect of PADs becomes more clear. The PADs of high-order ATI peaks tend to be peaked along the polarization vector, which is more obvious for higher-order peaks. We also notice that the PADs of higher-order peaks in circularly polarized fields are relatively slimmer than those of lower-order peaks, as shown in Figs. 2 and 3, which can be regarded as the broadening effect in circular-polarization case.

The broadening effect in the PADs provides an important reference to the CE control on the motion of photoelectrons. Because one of the aims of the CE control is to manipulate the motion of the ejected electrons as accurate as possible, if the PADs take up a broad range, the manipulations will be of lower efficiency. The broadening effect of the lower-order peaks indicates that an effective CE control is expected to be performed on the electrons of high kinetic energy.

IV. CONCLUSIONS AND DISCUSSIONS

In the frame of a nonperturbative scattering theory, the ionization of xenon atoms in a bichromatic phase-controlled field is studied and the dependence of PADs on the phase difference, the laser intensity and polarization, and the kinetic energy of photoelectrons are obtained. We conclude as follows: First, the PADs in the bichromatic field are inversion asymmetric, which is caused by the interference among different channels; second, in circularly polarized fields, the maximum of PADs keeps constant for various CE phases, but the position of maximal ionization rate varies with CE phase; although inversion asymmetric, the PADs are symmetric about an axis related to the CE phase; third, in linearly polarized fields, the maximal ionization rate varies with CE phase, but the PADs are always symmetric about the polarization vector; and finally, by investigating the broadening effect in the PADs of lower-order peaks, we show one can perform an effective CE control on the motion of electrons of high kinetic energy.

The electric field of the synthesized laser comprises an infinite sequence of identical, one-cycle laser pulses. Our studies show that one can perform an effective CE control by properly choosing the phase difference between two laser modes. This method is expected to be extended to other atomic processes. We notice that by means of the f -to- $2f$ interferometer technique, the CE phase of the short pulse can be stabilized within 0.1π [16]. Compared with the complicated phase-stable technique, the CE phase of the short-pulse sequences constructed by the multimode laser field is fixed and can be easily controlled. However, the electron wave packet ionized by the multimode laser field comes from many cycles, which differs from that by the ordinary few-

cycle laser pulses and the broadening of ATI peaks disappears.

When the duration of a short pulse is less than one optical periodicity, the concept of carrier and envelope fails to describe the short pulse, because the amplitude of low-frequency spectral components of pulsed radiation is not invariant under a phase transformation [15]. We notice that the pulse duration defined as the full width at half maximum of a single one-cycle pulse is even less than a half cycle, thus a single one-cycle pulse cannot be described by Eq. (1). While in our treatment of the one-cycle pulses sequence, the spec-

tral components of the laser field just includes the carrier frequency and its second harmonic, and low frequencies dismiss due to destructive interference.

ACKNOWLEDGMENTS

This work was supported by the Chinese National Natural Science Foundation under Grant Nos. 10234030 and 60178014, and National Key Basic Special Research Foundation under Grant No. G1999075200.

-
- [1] P. Agostini, F. Fabre, G. Mainfray, and N. Rahman, *Phys. Rev. Lett.* **42**, 1127 (1979).
- [2] P. H. Bucksbaum, D. W. Schumacher, and M. Bashkansky, *Phys. Rev. Lett.* **61**, 1182 (1988).
- [3] D. S. Guo and G. W. F. Drake, *Phys. Rev. A* **45**, 6622 (1992).
- [4] M. Bashkansky, P. H. Bucksbaum, and D. W. Schumacher, *Phys. Rev. Lett.* **60**, 2458 (1988).
- [5] S. Basile, F. Trombetta, and G. Ferrante, *Phys. Rev. Lett.* **61**, 2435 (1988); P. Krstic and M. H. Mittleman, *Phys. Rev. A* **44**, 5938 (1991).
- [6] G. G. Paulus, F. Grasbon, H. Walther, P. Villoresi, M. Nisoli, S. Stagira, E. Priori, and S. De Silvestri, *Nature (London)* **414**, 182 (2001).
- [7] D. B. Milosevic, G. G. Paulus, and W. Becker, *Phys. Rev. Lett.* **89**, 153001 (2002).
- [8] G. G. Paulus, W. Becker, and H. Walther, *Phys. Rev. A* **52**, 4043 (1995).
- [9] Lianghui Gao, Xiaofeng Li, Panming Fu, and Dong-Sheng Guo, *Phys. Rev. A* **58**, 3807 (1998).
- [10] T. Cheng, J. Liu, and S. Chen, *Phys. Rev. A* **59**, 1451 (1999); J. Chen, J. Liu, and S. Chen, *ibid.* **61**, 033402 (2000).
- [11] S. Watanabe, K. Kodo, Y. Nabekawa, A. Sagisaka, and Y. Kobayashi, *Phys. Rev. Lett.* **73**, 2692 (1994).
- [12] D. W. Schumacher, F. Weihe, H. G. Muller, and P. H. Bucksbaum, *Phys. Rev. Lett.* **73**, 1344 (1994).
- [13] D. W. Schumacher and P. H. Bucksbaum, *Phys. Rev. A* **54**, 4271 (1996).
- [14] M. Nisoli, S. De Silvestri, O. Svelto, R. Szipcs, K. Ferencz, Ch. Spielmann, S. Sartania, and F. Krausz, *Opt. Lett.* **22**, 522 (1997).
- [15] T. Brabec and F. Krausz, *Rev. Mod. Phys.* **72**, 545 (2000).
- [16] A. Baltuska, Th. Udem, M. Uiberacker, M. Hentschel, E. Goullermakis, Ch. Gohle, R. Holzwarth, V. S. Yakovlev, A. Scrinzi, T. W. Hansch, and F. Krausz, *Nature (London)* **421**, 611 (2003).
- [17] Jingtao Zhang and Zhizhan Xu, *Phys. Rev. A* **68**, 013402 (2003).
- [18] D.-S. Guo, T. Aberg, and B. Crasemann, *Phys. Rev. A* **40**, 4997 (1989).
- [19] F. Grasbon, G. G. Paulus, H. Walther, P. Villoresi, G. Sansone, S. Stagira, M. Nisoli, and S. De Silvestri, *Phys. Rev. Lett.* **91**, 173003 (2003).
- [20] Jingtao Zhang, Wenqi Zhang, Zhizhan Xu, Xiaofeng Li, Panming Fu, Dong-Sheng Guo, and R. R. Freeman, *J. Phys. B* **35**, 4809 (2002).
- [21] R. R. Freeman, T. J. McIlrath, P. H. Bucksbaum, and M. Bashkansky, *Phys. Rev. Lett.* **57**, 3156 (1986).